Chapter 10
Approaches for a Closer Look at Problems of Liquid Membranes with Amyloid-Beta Peptides

Tomáš Kondela, Pavol Hrubovčák, Dmitry Soloviov, Dina Badreeva, Tatiana Murugova, Vadim Skoi, Alexander Kuklin, Oleksandr Ivankov, and Norbert Kučerka

Abstract Alzheimer's disease is a neurodegenerative brain disease, where pathological hallmarks are senile plaques consisting primarily of amyloid-beta peptides. The investigations, however, point out not only the importance of physico-chemical properties of peptides themselves, but the membranes as the targeting environment as well. Commensurately, the interrogation approaches are required to focus on

T. Kondela · P. Hrubovčák · D. Soloviov · T. Murugova · V. Skoi · A. Kuklin · O. Ivankov · N. Kučerka (✉)
Frank Laboratory of Neutron Physics, Joint Institute for Nuclear Research, Dubna, Russia
e-mail: kucerka@nf.jinr.ru

T. Kondela
e-mail: kondela@jinr.ru

D. Soloviov
e-mail: dmitrysoloviov@jinr.ru

T. Murugova
e-mail: murugova@jinr.ru

V. Skoi
e-mail: skoi.vv@phystech.edu

A. Kuklin
e-mail: kuklin@nf.jinr.ru

O. Ivankov
e-mail: ivankov@jinr.ru

T. Kondela
Department of Nuclear Physics and Biophysics, Comenius University in Bratislava, Bratislava, Slovakia

P. Hrubovčák
Department of Condensed Matter Physics, University of P. J. Šafárik in Košice, Košice, Slovakia

D. Soloviov · V. Skoi · A. Kuklin
Moscow Institute of Physics and Technology, Dolgoprudny, Russia

D. Soloviov · O. Ivankov
Institute for Safety Problems of Nuclear Power Plants NAS of Ukraine, Kyiv, Ukraine

L. Bulavin and N. Lebovka (eds.), *Soft Matter Systems for Biomedical Applications*, Springer Proceedings in Physics 266, https://doi.org/10.1007/978-3-030-80924-9_10

these systems at various length scales ranging from the submolecular and molecular levels relevant to the structures of peptides and/or membrane lipids locally, to the supermolecular levels covering the aggregates and large structures ensuing from the peptide-membrane interactions. In this chapter, we are summarizing the previous studies that look at complex model and biological membranes using a variety of experimental and theoretical methods based on, or complementing, the scattering techniques. We attempt to examine the effects modulated by the presence of Aβ peptides, and more importantly to determine the modes of interaction between membranes and peptides.

List of Abbreviations and Chemical Substances

Abbreviations

Aβ	amyloid-beta
AD	Alzheimer's disease
APP	amyloid precursor protein
INS	inelastic neutron scattering
IXS	inelastic X-ray scattering
MD	molecular dynamics
NMR	nuclear magnetic resonance
NR	neutron reflectometry
NSLD	neutron scattering length density
PUL	polyunsaturated lipids
REMD	replica-exchange molecular dynamics
ROS	reactive oxygen species
SAND	small angle neutron diffraction
SANS	small angle neutron scattering
ULV	unilamellar vesicle

Chemical Substances

DMPC	1,2-dimyristoyl-sn-glycero-3-phosphatidylcholine

D. Badreeva
Laboratory of Information Technologies, Joint Institute for Nuclear Research, Dubna, Russia
e-mail: badreeva@jinr.ru

N. Kučerka
Department of Physical Chemistry of Drugs, Faculty of Pharmacy, Comenius University in Bratislava, Bratislava, Slovakia

DOPC 1,2-dioleoyl-sn-glycero-3-phosphatidylcholine
DOPS 1,2-dioleoyl-sn-glycero-3-phosphatidylserine
DPPC 1,2-dipalmitoyl-sn-glycero-3-phosphatidylcholine
POPC 1-palmitoyl-2-oleoyl-glycero-3-phosphatidylcholine
POPE 1-palmitoyl-2-oleoyl-sn-glycero-3-phosphatidylethanolamine
POPS 1-palmitoyl-2-oleoyl-sn-glycero-3-phosphatidylserine

10.1 Introduction

Biological membrane is a compositionally complex and fairly dynamic structure fundamental to the function of cells and organelles. The membrane contains three main types of components: lipids, proteins, and carbohydrates. Actual amounts of these components however differ between various biomembranes. For example, the major lipid components of a plasma membrane are 21 mol% phosphatidylcholine, 29 mol% phosphatidylethanolamine and phosphatidylserine, 21 mol% sphingomyelin, and 26 mol% cholesterol [1]. All the phospholipids are polar molecules, which in the presence of polar liquid form specific structures. Hydrophobic parts made up of long hydrocarbon chains move away from polar liquid, while lipid heads, in contrary, move towards the liquid in inter- and outer-cellular environments. This ensues forming the bilayered membrane. It is now generally accepted that active functions such as transport and signaling that take place at membranes are provided by the membrane proteins. Their proper function in turn depends on the physical properties of environment the proteins reside in, the underlying matrix made of lipids [2].

In general, the different membranes serve different functions and consequently have different structural properties. Indeed, the myriad processes taking place in these membranes are reflected in the lipidome's size and diversity [3]. For example, the thermodynamic phase of lipids plays one of the starring roles in determining the membrane's structural properties [4]. At the assistance of increasing temperature, the crystalline phase passes from a highly ordered structure to the liquid-crystalline phase typical of high disorder [5]. It is a lipid membrane in this fluid phase that is biologically most attractive due to its dynamic structure, in which the lipids almost freely diffuse yet embrace their overall bilayered structure of liquid membrane [6]. In addition to the temperature factor and participation of given lipids themselves, the membrane thermodynamic phase is determined by the presence of other membrane components. This is documented well in the case of cholesterol, whose concentration variation across the organelles gives the liquid membranes control over their structure and dynamics [7].

The changes of membrane functionality most likely originate in the structural properties of membrane, that are known to be accompanied by the changes in membrane physico-chemical properties. The cholesterol, for instance, increases the order of lipid hydrocarbon chains and increases the stiffness of the membrane. On the other hand, melatonin was found to increase the fluidity of the membrane and counteracted the effect of cholesterol [8]. Interestingly, decreasing levels of melatonin in the brain tissue were correlated with the aging similarly yet in a counteracting way

as increasing levels of cholesterol [9]. The role of membrane properties, its chemical composition, and additives is thus not surprisingly discussed in a connection not only to the membrane function but the disfunction too [10]. This concerns many various diseases, and those related to aging (amyloid toxicity and conformational diseases) in particular [11]. The crucial role in these processes is thought to be imparted by peptide-membrane interactions, which modulated by a membrane composition may cause a peptide to misfold and bring about irreversible conformational changes to other peptides and proteins.

Among conformational diseases, Alzheimer's disease (AD) is a neurodegenerative brain disease manifested by the nerve cell loss, which is the most common cause of dementia. Dementia is a clinical syndrome that can be characterized through the following symptoms: memory and speech disorders, later impairment of cognitive, intellectual, and physical abilities. AD affects 6% of the population over the age of 65 and its incidence increases with increasing age. It is estimated that 47 million people around the world suffer from dementia. Unfortunately, with a ubiquitously increasing aging of the population, this number will increase further, projected to reach 131 million in 2050 [12]. It was discovered in 1906 by Dr. Alois Alzheimer, who first observed morphological and histological changes in the brain of impaired patients [13]. He described amyloid plaques and the neurofibrillary tangles based on the autopsy observations. These two findings are still considered to be the main sequelae of the disease that are visible on the brain. The root cause of the disease, however, eludes explanations to the present days.

There have been several hypotheses suggested before 2019 [14] that try to explain the origin of AD (Fig. 10.1). Metal ions that play various functional roles in organisms, for instance, have been reported to participate in amyloid-beta (Aβ) peptide

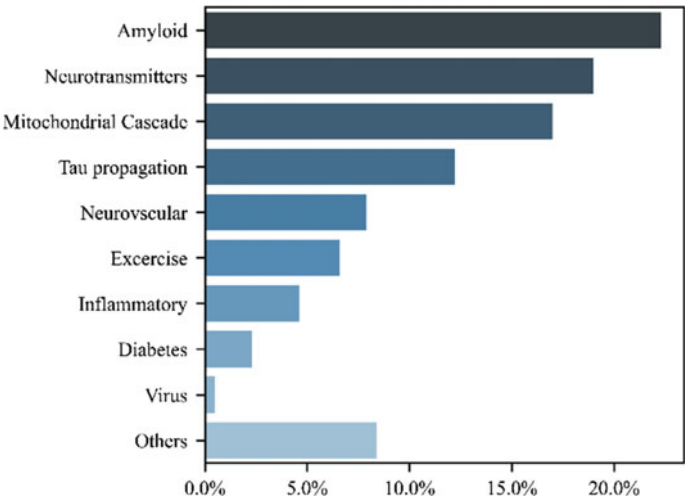

Fig. 10.1 Distribution of clinical trials performed with regards to the various hypotheses of AD up to the year 2019

aggregation and toxicity [15–17]. The most intriguing, however, are the cholinergic or neurotransmitters hypothesis [18], tau hypothesis [19], and Aβ hypothesis [20]. The cholinergic hypothesis is the oldest, based on the assumption that the cause of the disease is an insufficient synthesis of acetylcholine in the body, which serves as a neurotransmitter. Unfortunately, treatment with drugs that increase acetylcholine production has been shown ineffective [21].

The tau hypothesis identifies the tau protein situated inside the cell as a main contributor to the disease. The normal function of this protein is securing the division and orientation of cellular organelles in the underlying cytoplasm by creating a cytoskeleton system. These microtubes are then disrupted and gradually disintegrated as a result of the protein aggregation, leading eventually to the collapse of the cytoskeleton and subsequent disruption of the neuronal transport system, ultimately resulting in cell death. An anticipated trigger for the aggregation is Aβ peptides, though the details of this process are yet to be known [22–24].

Aβ peptides are proposed to be a key factor also in another hypothesis. It was first postulated in 1991 and it presumes that extracellular Aβ peptides form plaques that are a major cause of AD [20]. Aβ is a peptide that is most often composed of 40–42 amino acids. Its toxicity is associated with the fact that it aggregates into soluble oligomers, which may exist in several forms. It was suggested that a specifically misfolded oligomer may trigger other oligomers to take its form, generating thus a chain reaction and the formation of plaques and fibrils, which may supposedly be a cause of the disease [22, 25]. Recent studies are however more focusing on a monomeric Aβ and small oligomers as an origin of the AD [26, 27].

Aβ peptide is formed by enzymatic cleavage of amyloid precursor protein (APP) in two isoforms 1–40 and 1–42. APP is cleaved in two ways, the so-called non-amyloidogenic and amyloidogenic pathways [28, 29] (Fig. 10.2). The natural function of Aβ is not yet fully understood, although animal studies have not shown any significant physiological function [30]. Nevertheless, some potential activities such as regulation of cholesterol transport [31], enzyme kinase activation [32], or antimicrobial properties [33] have been discovered. As mentioned above, Aβ is most commonly associated with AD where it creates so-called plaques. It has been shown that in the early stages, the non-aggregated form of Aβ can penetrate the cell membrane and initiate intracellular toxicity mechanisms resulting in programmed cell death [34, 35]. As mentioned above, AD is a neurodegenerative brain disease, where about 50% of the brain's dry weight is supplied by lipids that support various structural or metabolic functions [36]. However, the lipids of different shapes and sizes do not affect the static structure only, but their different chemical composition modulates also the elasto-mechanical properties of the membrane. The liquid nature of membrane reflected in its fluidity is one of the examples that has been a topic of a vast number of studies [37–42]. Small molecules such as cholesterol and melatonin may alter the properties of liquid membrane further and in turn affect, in both diseases aiding or normal function protecting ways, amyloid fibril formation and toxicity. The intramembrane interactions become thus obviously a key factor in these hypotheses. One of the parameters proven to play an intriguing role in the interactions of Aβ peptide with membranes was concluded to be connected to

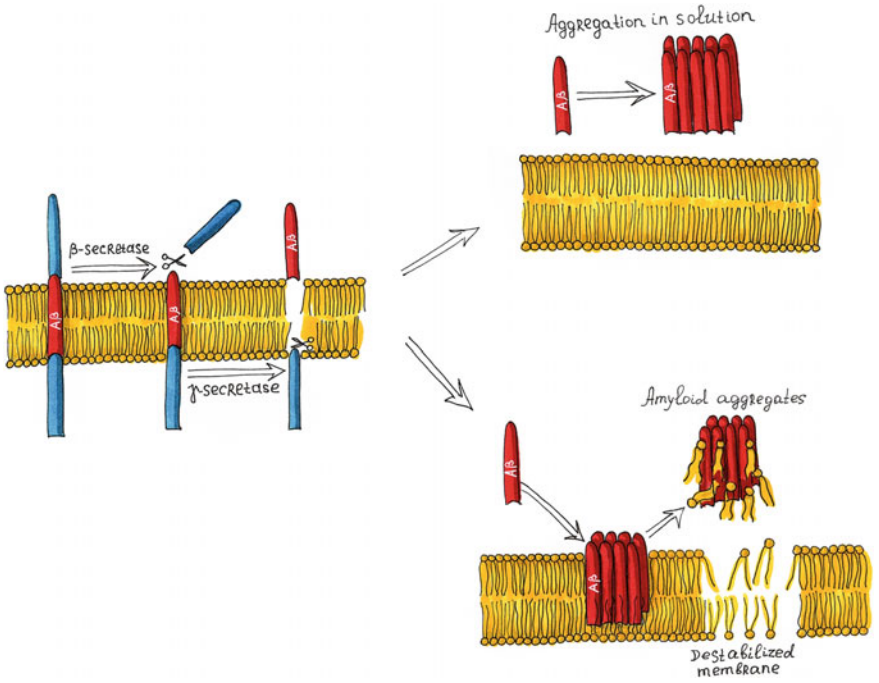

Fig. 10.2 The sketch of the amyloid-beta hypothesis of the Alzheimer's disease onset. The intermembrane amyloid precursor protein is cleaved in the amyloidogenic pathway, where extramembranous β-secretase and intramembranous γ-secretase cut APP to form $A\beta_{40}$ or $A\beta_{42}$ peptides. Created peptides may start to aggregate inside or outside the membrane in the case of misfolding conditions

the thermodynamic phase of lipid membrane. Apparently, $A\beta_{1\text{-}40}$ interact with the membrane at temperatures below the main phase transition due to the smoothness of tightly packed gel-phase lipids [43].

Other parameters of importance are the charge and pH. In mostly a zwitterionic lipid bilayer, the peptide will interact with the membrane interface while moving towards its hydrophobic core and thus it will prevent interactions with other peptides that can potentially trigger a change in its secondary structure. In the case of an anionic bilayer, the peptide will be more prone to interact with other peptides as it will be located closer to the membrane surface and exposed to the surrounding solution. The latter is more likely to contribute to oligomerization [44]. Also, a lower pH (pH ~ 5) can induce a more rapid fibrilization of amyloid-beta peptide [45], which means that a local decrease of pH near the anionic lipid bilayer can also contribute to the peptide aggregation. Controversially however, the aggregation of $A\beta_{1\text{–}42}$ was proposed not to occur at pH < 5 and pH > 9.5, while it started rather between pH > 6 and <9.5 [46].

A further factor which can be an important element in the aggregation of Aβ is oxidative stress. It has been linked to AD and other age-related neurodegenerative

diseases connected to dementia. Interestingly, the Aβ protein itself has been shown to further advocate oxidative stress [47, 48], as the AD infected brain exhibits more oxidative damage than a normal brain [49], and the areas of a high concentration of Aβ have displayed an increased level of protein oxidation [50]. As has been mentioned before, the pathological hallmarks of AD are senile Aβ plaques aggregated together with metal ions like copper, iron, or zinc. These redox-active metal ions together with Aβ can, in turn, produce the reactive oxygen species (ROS). The ROS as highly reactive chemical molecules then contribute to oxidative damage of the nearby molecules of lipids, proteins, and Aβ peptides [51]. All these effects subsequently introduce some characteristic changes to the structural properties of the membrane, and can thus be revealed by the methods of structural investigation. Neutron scattering is one of such influential techniques whose access to the membrane physical properties (thickness, shape, localization, and others) can answer some questions related to the oxidation stress, the impact of charge and pH, and possibly many other factors setting on the AD.

The study of membranes started with the discovery of a microscope in the seventeenth century. It allowed recognizing its bilayered structure and permeable character [52]. The most detailed insights into the membrane structure however became available in the twentieth century with advancement of scientific research based on scattering approaches [11, 41, 53]. The neutron scattering techniques extend these possibilities further owing to the ability of studying the inhomogeneities in membranes, which can be composed of not only different lipids but also proteins and peptides. These inhomogeneities can be in both lateral and normal directions, and can be presented by lipid rafts or the aggregates of membrane-embedded peptides and proteins. The rafts contain lipids with specific properties that are different from the rest of the lipid pool, most often related to the different thermodynamic phases. The structural information about rafts and lateral inhomogeneities in general, can be obtained by appropriate deuteration of lipids and/or adjusting the H_2O/D_2O ratio in the solvent [11, 54–56].

The parameters relevant to Aβ related investigations point out not only the importance of physico-chemical properties of peptides themselves, but the membranes as the targeting environment as well. Commensurately, the interrogation approaches are required to focus on these systems at various length scales ranging from the submolecular and molecular levels relevant to the structures of peptides and/or membrane lipids locally, to the supermolecular levels covering the aggregates and large structures ensuing from the peptide-membrane interactions. There are a few methods that allow to look closely at the membrane and interrogate these systems, that we will discuss in further details.

In this chapter, we are summarizing the previous studies that looked at complex model and biological membranes using a variety of experimental methods based on, or complementing, the scattering techniques. We pay special attention to those researching the possibility to regulate the membrane fluidity by regulating membrane chemical composition. Finally, we attempt to examine further how these effects are modulated by the presence of Aβ peptides, and more importantly how these effects determine the interactions between membranes and peptides.

10.2 Membrane Phase Transitions

Biological activities of the membrane surface-active compounds are known to depend on the chemical composition of lipid hydrocarbon chains, polar headgroups, and their capacity to attract water, and on the combination of lipids, cholesterol, melatonin, proteins etc. Indeed, as a function is often tightly coupled to the structure, the myriad specific functions occurring in these membranes are reflected in its compositional diversity. The multicomponent lipid mixtures allow the membrane, in the first place, to take control over its local thermodynamic phase.

A thermodynamic phase is a homogeneous property of a system, that is, a body defined by the same thermodynamic properties at its every point and without the dependence on the amount of matter. The different phases though may coexist while being separated from each other by interfaces. Phase transitions are common for all types of matter and are relatively well described theoretically. When external conditions such as temperature or pressure change, the phases can change from one to another [57]. This process is called a phase transformation, or a phase transition. A characteristic feature of the phase transition is a sharp change in the properties of the substance–for lipid structures, this means for example a change in the lateral diffusion rate by a factor of hundreds or even thousands. In turn, this is of key importance in life sciences. Indeed, the rate of exchange between the cell's comparative and external regulators of the multicellular organism will depend on the rate of diffusion.

The diffusion rates in membrane systems correlate closely with their thermodynamic state due to the balance of intra-membrane forces that in turn depends on thermodynamic conditions. This delicate balance of forces is responsible for minimizing the system's total energy and includes both headgroup and hydrocarbon chain interactions manifested mostly by the attractive hydrophobic forces within the hydrocarbon chain region and headgroup dipolar interactions, and the repulsive steric and entropic effects. When following the consequences of temperature changes, there is an additional factor giving rise to another essential interaction within the lipid membrane, namely trans-gauche isomerization. The probability of trans-gauche isomerization in acyl chains increases with increasing temperature and has the opposite effect to that of van der Waals force. Most importantly however, it introduces the disorder within the hydrocarbon chain region and induces the membrane softening. This has proven a determinant feature in many phenomena in the vicinity of chain-melting phase transition [58].

By the early 1970s, as a result of studies mainly carried out by the method of X-ray structural analysis, it was found that water–lipid systems form a wide range of liquid crystal phases [59]. It was found that lamellar lipid phases, to which the phases of real cell membranes belong, are usually smectic according to Friedel's classification. These phases include the so-called L_β gel phase and L_α fluid phase, corresponding to the thermodynamic state of lipids in a living cell. The phase transition from gel to fluid is called the main phase transition. Its study in model membranes of various compositions was considered to be an important task, particularly in the studies of

lipid membranes doped with Aβ peptides, since the phase state of the lipid membrane can also influence the localization of peptides [43].

The lipid membranes are characterized by lyotropic mesomorphism (dependence of the state on lipid headgroup hydration) and thermotropic mesomorphism (dependence of the structure on temperature) [60]. Both properties are related. The main phase transition of lipids occurs at a characteristic temperature T_m, the value of which depends on the water content in the system. Temperature of the phase transition reaches a minimum as soon as the total water content exceeds the amount that can bind lipid structures. At the same time, lipids with a lack of water can be in an ordered state even at temperatures above T_m.

For the studies of systems with lipids and Aβ peptides, it is important to mention the traditional classification of the phase transitions of the first and second order. According to Landau's theory [61], during the phase transitions of the first kind, the distribution function of the system must be bimodal in the vicinity of the phase transition point, that is, it must have two maxima. The highest maximum corresponds to the most stable state of the system, and the second maximum corresponds to a less favorable, metastable state. At the very transition point, the heights of the maxima become the same, and the system can simultaneously coexist in both states. In second-order phase transitions, the distribution function has always only one maximum, which changes discretely at the transition point. Accordingly, in the case of second-order transitions, metastable states do not exist.

One of the characteristics of the lipid bilayer, that allows determining the transition from one phase to another is its mass density ρ. In the case of water–lipid systems, ρ means the macroscopic density of the system, whose changes depend on the system volume V only. The coefficient of its thermal expansion (at constant pressure p) can be expressed in terms of the volume change (dV) due to the change of temperature (dT) [62]:

$$\alpha_p = \frac{1}{V}\left(\frac{\partial V}{\partial T}\right)_p \tag{10.1}$$

During the first-order phase transitions, α_p turns to be infinite in the vicinity of phase transition temperature and during the second-order phase transitions, it experiences a jump. Conveniently thus, one can determine the system phase transition by the volume dependence on temperature. This allows the densitometry method to be used to determine the thermodynamic phase of lipids and the characteristics of their main phase transition [63].

One of the modern methods for determining the density of liquid and gaseous samples is densitometry based on the Pulsed Excitation Method [64]. The principle is based on determining the period of forced vibrations of a tube filled with a sample. In this case, the oscillation period τ is related to the density ρ of the sample filling the tube by the simple relation:

$$\rho = A\tau^2 - B \tag{10.2}$$

where A and B are instrumental constants. Among the existing measuring tube configurations, U-shaped tubes are often used for highly accurate determination of the density of liquid samples with 5-digit accuracy (e.g., DMA densitometers by Anton-Paar, Graz, Austria). Oscillations of such a system occur in a direction perpendicular to the plane of the tube, allowing also for a high precision temperature control. Some disadvantages of the described method on the other hand, include the relatively large sample volume required (about 1 ml), as well as the possibility of its macroscopic separation during long-term measurements. The latter can be avoided by the periodic re-homogenization of the sample [65].

In addition to temperature and pressure, the phase state of lipid membranes can be influenced by the presence of ions, or low and high molecular weight compounds. The above described instrumental method has been utilized recently for example in determining the temperature and width of the main phase transition of lipid bilayers with the addition of cholesterol and melatonin [66]. These can be determined readily from the graph of first derivatives $d\rho/dT$ (see Fig. 10.3). The results have shown that the presence of melatonin and cholesterol dramatically shifts the position and width of the peak of the density first derivative, which turns out to be in accordance with their known influence on the membrane thermodynamic phase.

The fluidizing effect of melatonin can be concluded based on shifting the membrane thermodynamics towards the fluid phase. The mechanism of the effect has been speculated to be linked to the incorporation of melatonin in the head group region, introducing thus the defects in the hydrocarbon region. On the other hand, the effect of cholesterol turned out to be in removing the gel-to-fluid phase transition detected for the neat lipid system previously. This is in good agreement with the

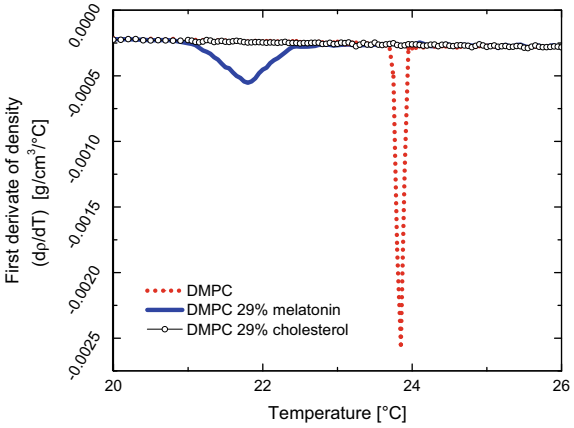

Fig. 10.3 The dependencies of the first derivative of mass density vs temperature for 1,2-dimyristoyl-sn-glycero-3-phosphocholine (DMPC) multilayer vesicles aqueous dispersion (error bars are smaller than the symbol size). A sharp peak corresponding to the main gel-to-liquid phase transition is observed for pure DMPC (red). For DMPC with the addition of melatonin, the peak position and shape change significantly (blue). For DMPC with the addition of cholesterol, the peak vanishes completely (black circles)

formation of cholesterol-induced liquid ordered (Lo) phase, in which the membrane is fluid even below the phase transition temperature of lipid. In an aim to understand the systems at high cholesterol concentrations, the presumed cholesterol's ordering effect on the lipid chains and the overall membrane structure has to be scrutinized further by other experimental techniques, such as those based on scattering principles.

10.3 Overall Membrane Thickness

Small angle neutron scattering (SANS) is a powerful technique for studying the structure of membranes, such as lipidic model membranes and biological membranes isolated from alive systems. Its main advantage comes from the possibility to measure samples in biologically relevant conditions, and in retrieving structural characteristics on several length scales. SANS gives some essential information about the overall size of objects on the level of thousands of angstroms, at the same time with the thickness, curvature, inhomogeneity, and asymmetry of the membrane on the level of tens of angstroms.

The membrane-containing samples for SANS mainly present liquid dispersions, in which the solution is typically made deuterium rich for enhancing the neutron scattering contrast between the membrane and solution. While biological membranes need to be extracted according to the particular protocols required for their isolation, it is desirable to use the heavy water buffers in the final steps. If the membranes are formed by synthetic lipids, the lipid powders or films are dispersed in D_2O-based buffers initially. For multicomponent model membranes, all components are pre-dissolved in an organic solvent (chloroform, methanol, trifluoro-ethanol, or their mixtures). That allows one to achieve a homogeneous mixing of all components, at the same time as it enforces the efficacy of the incorporation of various transmembrane components, such as proteins and peptides. The protocols for embedding Aβ peptide into model membranes have their specifics that can be found elsewhere [11, 67]. All components (in desired ratios and after receiving required pre-treatments) are thus mixed in glass tubes, and the solvent is evaporated by a nitrogen stream and subsequent evacuation. The resulting film that forms on the walls of the glass tube is then hydrated with D_2O or D_2O/H_2O mixture to obtain the membrane concentration of about 1 wt% that is required by SANS measurements.

In the case of most commonly used lipids mixed with water, they tend to spontaneously form large multilayered vesicles. These objects result in strong diffraction patterns when examined by neutron (and/or X-ray) scattering. Although the diffraction patterns have their advantages and are successfully employed in various structural studies, they overwhelm the smooth scattering signal due to the membrane inner structure [68]. Therefore, the multilamellar vesicles are often extruded through polycarbonate filters with pores of 300–1000 Å to break the multilayers into unilamellar vesicles (ULVs), and to unify them in size. The prepared samples are typically poured into quartz cuvettes and placed in a specialized thermo-holder [69].

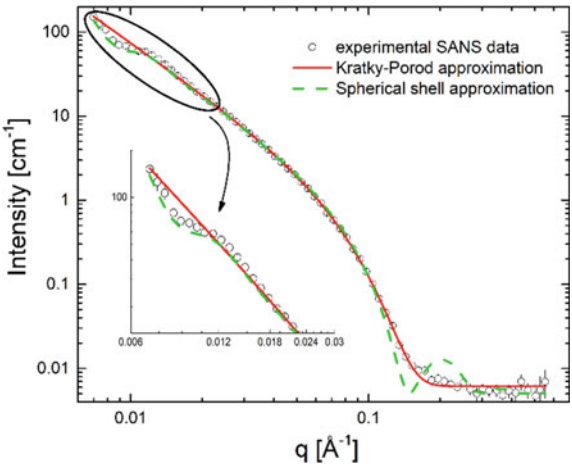

Fig. 10.4 SANS curve for lipid ULVs with embedded $A\beta_{25–35}$ peptide. The Kratky-Porod approximation is superior for extracting membrane thickness as seen by its close fitting to the curve in the high q region, while the spherical shell approximation improves the fitting in the low q region that corresponds to the overall vesicle parameters as demonstrated in the insert

The experimentally measured SANS curve in the case of non-interacting ULVs is typically smooth and almost featureless. It remains true after the addition of peptides if their fraction in the membrane is small enough to prevent aggregation or other specific inter-lamellar interactions. The analysis of the experimental data can then be carried out in a manner that is used for lipid membrane systems. The example of the experimental SANS curve and its theoretical approximations are presented in Fig. 10.4.

The simplest way to calculate membrane thickness is according to Kratky-Porod approximation for a region of medium scattering vectors ($0.02 < q < 0.1$ Å^{-1}):

$$I(q) = \frac{A}{q^2} \cdot e^{-q^2 \cdot R_t^2} + b \tag{10.3}$$

where q is a scattering vector defined as $4\pi \sin\theta/\lambda$, θ is the angle of incident and λ is the neutron wavelength; A is a constant depending on the average scattering length density, volume, and quantity of membranes in an experimental sample; b is a scattering background; and R_t is a radius of gyration along the thickness of a membrane. The latter relates to the membrane thickness as $d = \sqrt{12} \cdot R_t$. In this case, the membrane is supposed to have a homogeneous distribution of scattering length density. The function (Eq. 10.3) is simple and unambiguous. The shape of the theoretical scattering curve depends only on value R_t and does not depend on the size and overall shape of the membrane. The example of the approximation is presented in Fig. 10.4. This approach is widely used to study the effect of various factors on membrane thickness [70], including the presence of Aβ peptides [66].

There is however additional information readily obtainable from SANS experiments that relates to the overall form and size of objects. Since model and biological membranes in solution tend to form vesicles, their scattering curves can be approximated by function for spherical shells:

$$I(q) = \frac{A}{q} \cdot [(R+T)^2 j_1(q(R+T)) - R^2 j_1(qR)]^2 + b, \tag{10.4}$$

where $j_1(x) = \frac{\sin x}{x^2} - \frac{\cos x}{x}$ is the first-order spherical Bessel function, R–is the inner radius of a shell, T is the thickness of a membrane, A is a constant depending on membrane concentration and contrast between membrane and solvent.

The function assumes that the scattering length density of the membrane is uniform, which however, can be improved easily by introducing more sophisticated models [71]. In addition, Eq. 10.4 has to be convoluted further with the size distribution function depending on radius R, due to the size polydispersity of real ULV samples [71].

Among the other studies, SANS allowed us to study the effect of cholesterol and melatonin on the membrane parameters in the presence of Aβ peptide, and the regime of peptide interactions with the membrane [66]. In the case of single lipid membranes, cholesterol makes the membrane thicker due to its "condensing effect" that increases the ordering and consequently the length of lipid tails. Melatonin, on the other hand, reduces the membrane thickness because of its disordering effect on lipid tails. Thus, cholesterol and melatonin can regulate the membrane fluidity in opposite directions: cholesterol decreasing, and melatonin increasing, as suggested already by the results of densitometry.

Importantly, both cholesterol and melatonin are present in the brain where they are believed to regulate the binding of Aβ peptide with membrane, and to affect the amyloid fibril formation [72, 73]. Our further SANS experiments have indeed shown the incorporation of Aβ peptide into the phospholipid membrane [66]. In the case of a pure lipid membrane, the peptide induces the thinning of the membrane. This effect can indicate that the peptide binds to the lipid-water interface of the bilayer, thereby increasing disorder in the bilayer and shortening the lipid tails, similarly to the case of the addition of melatonin. The same thickness behavior was observed upon the addition of Aβ peptide into the cholesterol containing membranes. In the case of melatonin containing membranes, the thickness change was negligibly small. That can be explained by the peptide incorporation into the hydrocarbon chain region as outlined in Fig. 10.5. It may be noted however, that the speculated results are at the limit of SANS experiments, and the approaches providing higher resolution are in place for further confirmation.

10.4 Detailed Membrane Structure

While the above discussed experimental approach of SANS covers several length scale regimes, it is nevertheless a low-resolution method with the limitation on the level of tens of angstroms (corresponding roughly to $2\pi/q_{max}$, where a typical $q_{max} \sim 0.2–0.3$ Å^{-1}). This satisfies the information related to the overall membrane properties. It is however not possible to look more closely at the membrane local structure and even submolecular arrangements. The extension of the high-resolution limit is

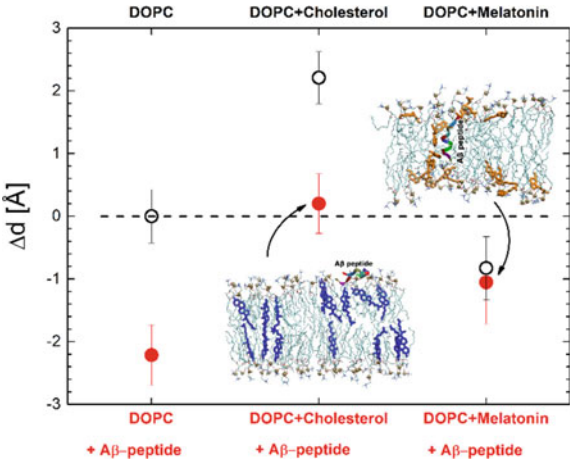

Fig. 10.5 The changes in the thickness of DOPC bilayer Δd induced by the incorporation of Aβ peptide at the presence of cholesterol or melatonin [66]. The thickness of pure DOPC membrane was taken as a reference point (dashed line). The black empty points and top axis correspond to DOPC bilayer without Aβ peptide, and the red points and bottom axis correspond to the DOPC bilayer with 3 mol% of Aβ peptide. The inserts contain snapshots of molecular dynamic simulations of corresponding systems, corroborating the peptide's location near the lipid-water interface in the case of pure DOPC and that with the addition of cholesterol, while it is localized in the hydrocarbon region in the case of melatonin addition

often possible thanks to the changing the geometry of samples from unilamellar to multilamellar membranes, and from unoriented spherical vesicles to the parallelly oriented arrays [68]. As a result, several diffraction orders that become achievable experimentally may provide a spatial resolution of several angstroms (typical q_{max} ~ 0.6–0.8 $Å^{-1}$).

Similarly to SANS, small angle neutron diffraction (SAND) measurements are performed in an inverse *q*-space followed by the reconstruction of neutron scattering length density (NSLD) profiles in a real space. This is achieved straightforwardly through the Fourier transform of diffraction form factors F_h (calculated as a square root of integral diffraction intensity) [74]:

$$NLSD(z) = \frac{2}{D}\sum_{h=1}^{h_{\max}} F_h \cos\left(\frac{2\pi hz}{D}\right) \tag{10.5}$$

where *h* is a peak order, and *D* is a lattice spacing calculated from the Bragg equation. In this, neutron diffraction in particular provides an unprecedented possibility to solve the infamous scattering phase problem directly in the experiment. The phase signs (+ or – for centro-symmetric systems in the case of most membranes) of diffraction form factors can be deduced from the systematic substitution of H_2O by D_2O in the hydrating solution that must yield a linear change as a function of D_2O fraction [74].

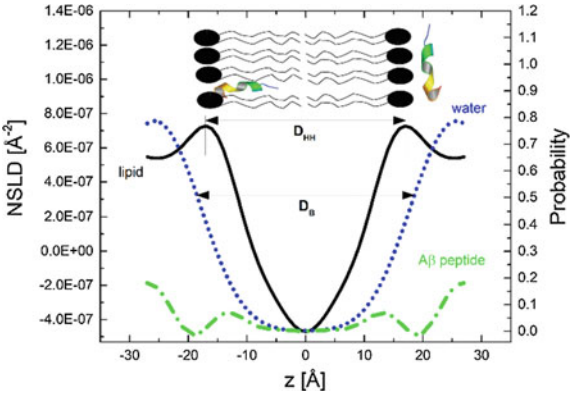

Fig. 10.6 The NSLD profile reconstructed from SAND experiment. The solid line scaled to the left-hand axis shows the total NSLD profile of the entire bilayer hydrated with 8% D2O. The broken lines scaled according to the right-hand axis show the probability distributions of water (blue color) and 3 mol% Aβ peptide (green color). The insert on top of the graph depicts schematically the plausible distributions of Aβ peptides within the bilayer

The NSLD profiles obtained at various D_2O concentrations are then utilized in determining several membrane structural properties. The profiles obtained at 8% D_2O solution, for example, show only the membrane not obscured by the scattering from solvent (see Fig. 10.6). This is because the neutron scattering length for H is –3.739 fm and that for D is 6.671 fm (together with 5.803 fm for O) [75], making the contribution of 8% D_2O water solution to the NSLD practically zero. These profiles are thus often used to extract lipid head-to-head thickness D_{HH} from peak to peak distance across the bilayer. The D_{HH} variations resulting from the compositional changes are then rudimentary parameters when looking for correlations between structure and function. The evaluation of D_{HH} allowed for example to postulate the condensing effect of cholesterol and fluidizing effect of melatonin [8], as discussed in the previous section on SANS and densitometry.

In order to better understand how various components affect the interactions of biomolecules with the membrane, it is necessary to determine also their location within the membrane. The SAND experiments allow just that by providing quantitative data on the distribution of structural moieties, their sizes, shapes, and correlation lengths. At first, these can be determined following the assumption that the given component does not disturb the overall structure of the membrane and rather changes its features locally. In fact, this approach can be easily applied not only to neutron techniques, but to the X-ray diffraction as well, assuming the additions are made in small quantities. For example, 1.5 mol% of Aβ peptide was localized either inside the membrane core or at its surface depending whether shortened or full length peptide was added, respectively [76]. Our recent results demonstrate this approach in Fig. 10.6.

Another important result attainable from SAND experiment while utilizing contrast varied NSLD profiles is the water probability profile (see Fig. 10.6). The

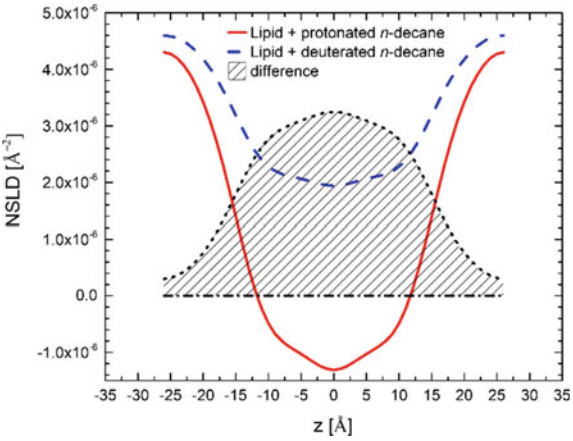

Fig. 10.7 The example of the NSLD profile difference of labeled (blue) and unlabeled (red) samples. The difference reveals the label distribution along the profile, whose integrated area under the curve is directly proportional to the amount of the label

general NSLD profile consists of the contribution due to lipid membrane (and its substances as melatonin, cholesterol etc.) and water. The subtraction of NSLD profiles measured at any two different D_2O contents provides thus the probability distribution of water only, as the unchanged membrane contributions cancel out each other [74]. The mean position of water-bilayer interface present in the water distribution (often obtained by error function fitting) determines then the bilayer thickness D_B (Fig. 10.6).

Finally, the most intriguing advantage of neutron diffraction and the contrast variation technique in particular, is the labeling approach. The sensitivity of neutrons to various membrane components can be changed similarly to the case of D_2O/H_2O exchange discussed above. The subtraction of the two NSLD profiles yields a distribution of label and thus a given moiety in question [77]. An example of this approach is illustrated in Fig. 10.7, where protonated vs. deuterated n-decane was added to the lipid membrane [78]. The differences are visible clearly when the labeled components are contained at high concentrations (up to 2:1 ratio of n-decane:lipid in the work mentioned). Unfortunately, often employed minute amounts of labeled components preclude the practicality of this approach in SANS and SAND methods. Its applicability may nevertheless benefit from even higher resolution achievable in reflectometry as we will discuss further.

10.5 Single Planar Membrane

Neutron reflectometry (NR) turned out to be a feasible tool for the investigation of model lipid membranes with the ever-progressing advancement of neutron sources. Particular attention has been paid to the application of NR for the study of interactions between the membranes and various proteins. Currently, there is a great expansion in its application also to the research of membranes with Aβ peptides, driven mainly by

two factors. The first is the wide evidence on the Aβ peptides aggregation at the cell membranes that is correlated with the pathology of many serious disorders including Alzheimer's, Parkinson's, and prion disease or type II diabetes [79, 80]. The second factor is a great effort behind the optimization of the sample preparation methods for the NR studies of biological processes. As a result, NR allows scrutinizing the submolecular details of single planar membranes. Despite the availability of other well-developed experimental methods with comparable resolution (e.g. SANS and SAND), the application of NR can provide structural information on the systems with a specific architecture.

The suitability of NR follows from the fundamental principles of reflectometry as an optical method designed for the examination of thin layers. At a certain level of generalization, a single lipid membrane can be treated as a system of parallel layers, hence appropriate for scrutinizing by the NR. In addition, the crucial difference with respect to other methods is that NR allows inspecting a lipid bilayer in its individual planar form. This is in a contrast to the diffraction experiments where adjacent bilayers in the stack may intercept or hinder the access of solvent (and additives) in-between the lamellae. Although SANS enables experiments with lipid bilayers in a single form, ULVs of spherical shape and significant curvature may also exhibit some limitations with respect to the concept of the cell membrane model. The drawbacks that have to be considered are the difference of lateral pressure in inner and outer bilayer leaflets as well as the actual thickness of the lamella.

From the fundamental point of view, NR probes the structure of thin homogeneous layers and their interfaces with a possible resolution down to a few angstroms. The lipid bilayer deposited onto an optically flat surface can be regarded as a system of such layers with corresponding refraction indices. Impinging neutron beam penetrates the sample and it is reflected at the interfaces according to the laws of optics. The neutron reflectivity, *R*, refers to the ratio of the incoming and exiting neutron beams (the ratio of elastically and specularly scattered neutrons to incident neutrons) and it is measured as a function of momentum transfer q (see the definition in 'Overall membrane thickness' section). *R(q)* is given by the Fresnel's law and Born approximation as the Fourier transform of *NSLD(z)* distribution in the direction perpendicular to the interface, similar to that in previous cases of SANS and SAND [81]:

$$R(q) = \frac{16\pi^2}{q^2}\left|\int NSLD(z)e^{-iqz}dz\right|^2 \tag{10.6}$$

Therefore, the intensity of the reflected beam depends on the thickness, density, and interface roughness of the sample.

Figure 10.8 shows reflectivity curves obtained for the single lipid bilayer systems deposited on a planar solid substrate. The influence of cholesterol (29 mol%), melatonin (29 mol%), and both compounds together (29 mol% + 29 mol%) on the structural properties of DOPC bilayer was investigated. The systems were hydrated by immersing the bilayer face of the substrate to heavy water (D_2O). Characteristic features of the *R(q)* curves are fringes with their magnitudes and local minima positions with respect to q. They relate to the layer's NSLDs and thicknesses in each system.

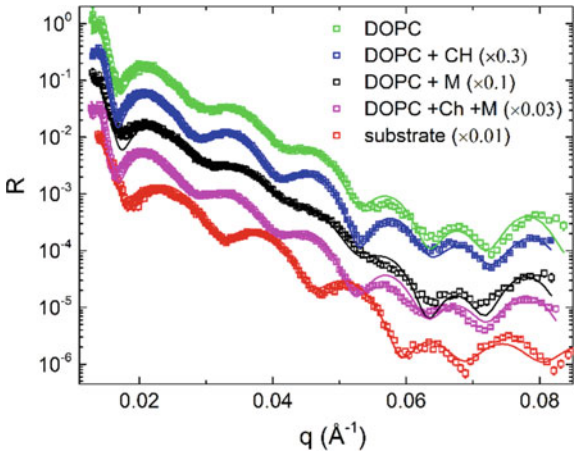

Fig. 10.8 NR data obtained for the DOPC bilayer (green), and systems composed of DOPC with the addition of 29 mol% cholesterol (blue) and melatonin (black) separately or together (29 mol% + 29 mol%, magenta). Solid lines represent the best model fits to the experimental data. The data are scaled according to the factors shown in the legend for enhancing the clarity of presentation

In order to obtain the NSLD profile of the system and hence to determine its composition along the normal to the surface, reflectivity curves are modeled and subsequently fitted to the experimental data. The models employ the approach where the *NSLD(z)* is decomposed in a finite series of layers, each of which is defined by three parameters: NSLD, thickness, and roughness. Roughness refers to the interface of two adjacent layers and it is usually expressed by error function. Some advanced models account for an extra parameter that reflects less than the complete coverage of the substrate by the membrane. The data shown in Fig. 10.8 were fitted by the use of a model that assumes a lipid bilayer composed of three homogenous slabs comprising the lipid heads, lipid tails, and another side lipid heads. The results obtained by NR for the examined single planar membranes were [107] found to corroborate the data reported above for the membranes in the form of multilayers or ULVs obtained using SAND and SANS techniques, respectively [8, 66]. The counteracting effect of cholesterol and melatonin on membrane thickness (increase vs decrease, respectively) has been reconfirmed. More intriguingly, the submolecular resolution of NR allows extending the research by identifying the positions of the two components and their effects on the incorporation of other bio-related membrane components.

In order to address the tremendous variability of lipid membranes and the biological processes they facilitate, several sample preparation methods for the examination of protein adsorption by different biomimetic model membranes have been developed and employed in NR. Currently, three general approaches are utilized most frequently, depending on specific conditions that are required to maintain in a given examined system. The most common types of biomimetic membranes they are expected to model are (i) phospholipid monolayer at air/water interface, (ii) phospholipid monolayer on solid supports, and (iii) fluid lipid bilayers on solid support. Monolayers at the air/water interface (i) provide advantages in their simplicity, stability, ease of preparation and controlling of their properties. Proteins are adsorbed to the monolayer from the aqueous phase, while the lipid packing density of the phospholipid

monolayer formed using the Langmuir trough can be precisely monitored by controlling the applied surface pressure. This ability is available even during the experiment and it is absent in the majority of other artificial membrane models. Its unique application potential stems from the fact that lipid packing density affects the protein or peptide interactions with membranes. It has been shown with the aid of NR that the amount of proteins associated with lipid monolayers decreases with the increase of surface pressure [82].

Instead of water, monolayers can be also spread on solid supports (ii). Since phospholipid monolayer mimics one leaflet of a biological membrane, it can be employed in the studies of the interactions and adsorption of peripheral proteins [83]. Finally, fluid lipid bilayers on a solid support (iii) represent the group of the most popular artificial membrane models. Unlike the lipid monolayers, they mimic the plasma membrane more accurately, hence being physiologically more relevant. In the wide range of their applications in NR, these systems have shown their suitability in the studies of protein-membrane interactions where the effect of bilayer environment has also been taken into account.

The foremost investigated environmental effect in membrane research is that determining the membrane thermodynamic state, in which the concept of lipid rafts is attracting a lot of attention. For example, the interaction of Aβ peptides with a single asymmetric complex membrane mimicking the lipid raft in its composition is suggested important for Aβ peptides settling and seeding [84]. NR with the aid of solvent contrast variation method, and contrast enhancement between deuterated lipids and hydrogen rich peptides was able to localize the place of action of the Aβ peptide structures and assess their penetration depth. Apparently, the structured oligomers of $A\beta_{1–42}$, considered as the most membrane-active state, are penetrating the outer leaflet of the membrane only, where they can serve as seeds for further Aβ aggregation. On the other hand, the unstructured $A\beta_{1–42}$ early-oligomers were localized even in the inner leaflet. Based on the peculiar NSLD profile, Aβ monomers are hypothesized to organize themselves within the membrane environment to form the pores.

A different approach is employed in the case of polymer cushioned membranes that are deposited on a soft polymeric layer. The layer provides an environment that attempts to mimic the cytoskeleton or extracellular matrix. It facilitates the reconstruction of membrane domains morphology and allows for mobility of the transmembrane proteins. In this way, the role of $A\beta_{1–42}$ peptides on polymer cushioned membranes with composition mimicking the neural membrane could has been studied at physiological conditions [79]. By monitoring the kinetics of the bilayer formation followed by the injection of Aβ peptides, the NR curves and consequently reconstructed NSLD profiles revealed the penetration of Aβ peptides to the membrane. This could have been correlated nicely with the concomitant increase of membrane thickness and softening. Although the membrane thickness is certainly one of the primary parameters achievable in NR (as well as SANS and SAND), the softening is a parameter related to the membrane dynamics, and is therefore best researched by other methods, including the inelastic scattering.

10.6 Membrane Dynamics

Inelastic X-ray and neutron scattering techniques (IXS and INS) are widely used to study the dynamic properties of various materials. The method is based on measuring the energy and momentum changes of photons (neutrons), which are determined by excitations of atoms and/or molecules (known as phonons) inside the sample. IXS method requires incident photons with energies $(10 \div 25)$ keV with transfer energies during scattering on a sample within $(1 \div 100)$ meV [85].

IXS and INS represent two of the few techniques capable to detect rotational and vibrational excitations of lipid molecules [86, 87], diffusion processes inside the membrane [88, 89], and to determine energies of intermolecular (lipid-lipid and lipid-protein) interactions in picosecond-nanometer time–space window [90, 91] in particular. IXS and INS are complementary techniques, with their advantages and disadvantages. For example, INS is nondestructive for the sample and provides excellent energy resolution, but has a limited dynamic range due to kinematic constraints. In contrast, IXS has no superior energy resolution (comparing to INS) and the lipid sample may be damaged by radiation during the experiment. At the same time however, IXS scattering cross-section is inherently coherent, so the deuteration of lipid tails (often performed for experiments with neutrons), which changes lipid's physical properties, is not required. This makes IXS method a bit more preferable for studying the dynamical properties of lipid membranes.

A typical spectrum of in-plane inelastic X-ray scattering on oriented lipid multilayers is shown in Fig. 10.9. In addition to the central elastic peak, which corresponds to a zero-energy transfer of incident photons, the IXS curve exhibits few inelastic peaks whose energies are determined by the energies of the corresponding propagating phonon modes. Positive and negative values of the transferred energy correspond to the creation and annihilation of phonon, respectively. The number of inelastic peaks is determined by the number of unique phonon modes. The dependences of transferred energies on the scattering vector q are called the dispersion curves. The range for the q vector is determined by the size of quasi-Brillouin zone, which can be understood as the mean distance between the hydrocarbon chains in the case of lipid membranes.

The IXS technique used recently for investigating the diffusion and relaxation processes occurring in the lipid membrane has provided experimental evidence for a dispersive transverse acoustic mode in both L_β and L_α phase of a pure dipalmitoylphosphatidylcholine (DPPC) that has not been reported before in the literature [90]. The transverse mode exhibited a low-frequency phonon gap when the DPPC transitions into the L_α phase. It was argued that such band gaps are directly related to spontaneous short-lived (on the picosecond timescale) local lipid clustering and, consequently, the formation of volume voids in the membrane. The void formation process then in turn appears to underlie the passive transport of small solutes through the cell membrane.

Further, the investigation of collective vibrations in DPPC-cholesterol binary mixtures has revealed the existence of an optical phonon, which emerges due to

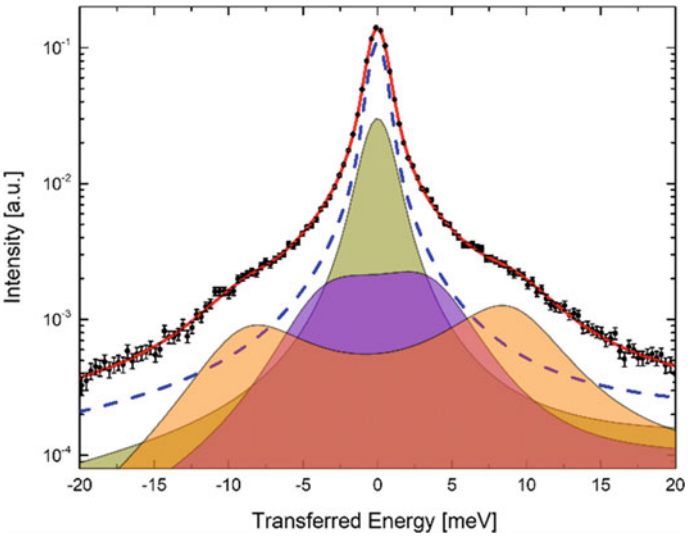

Fig. 10.9 A typical spectrum of in-plane inelastic X-Ray scattering on oriented lipid membranes (black points). The central elastic peak is shown by the blue dashed line, and several inelastic peaks are shown by lines with color filled regions

out-of-phase vibrations of coupled DPPC and cholesterol molecules [91]. The effect of cholesterol molar fraction on the phonon band gap opening and evolution has been determined. The opening of the optical phononic gap with increased cholesterol concentration is direct evidence of the nanoscale domains in Lo phase and their relationship to the mechanical properties of the cell membrane (such as surface tension, or bending rigidity), which in turn is related to various cell functions, like passive transport, cell curvature generation and sustainability.

Considering the recent interest in membrane complexes with cholesterol, melatonin, and Aβ peptides, it will be interesting to employ the above discussed approach in determining the effect of cholesterol and melatonin – separately as well as together – on the phonon band gap opening in model phospholipid membrane with Aβ peptide. Such a system may ensue a formation of rafts as already mentioned in previous sections. Conveniently, the formation of lateral inhomogeneities creates defects at the interfaces of these structures that can be well detected and characterized by inelastic scattering. The integration of peptides amid lipid molecules would also have a characteristic fingerprint in experimental data. The concentration and temperature studies of the phonon band gap evolution will shed a light on the role of cholesterol and melatonin in the considerable changes to the membrane structural properties. This will provide the base information for furthering our understanding of the processes like Aβ peptide insertion and lateral distribution, direct transport of small molecules, and energy transfers in cell membranes.

10.7 Aβ Peptide Secondary Structure

One of the main interests in the Aβ peptide related investigations is the mechanism of peptide incorporation into the biological membrane and/or its withdrawal from the membrane. This mechanism is expected to be influenced by both the membrane elasto-mechanical properties and structural properties of Aβ peptides. Although neither is understood yet fully, the quaternary structure of amyloid fibrils points the attention on the tertiary and secondary structures of Aβ peptides (not to discuss the importance of primary structure that is documented by the toxicity of Aβ peptides and their amino acids 25–35 in particular).

One of the methods for determining the secondary structure of peptides is circular dichroism. This method has been used since the very first investigation of the $A\beta_{25–35}$ peptide aggregation. The results showed a balance between the α-helical, β-sheet and random coil structures with the changes of various conditions [92]. The balance was shown to be pH dependent with the concentration driven transition of the random coil to β-sheet happening in sodium acetate buffer at pH 4 and 5.5, and it shifted the distribution towards the β-sheets with the increasing of pH up to 7.4. The addition of negatively charged lipid vesicles to the system comprising $A\beta_{25–35}$ also caused the distribution balance to shift in the direction of β-sheet formation, which could be obtained alternatively by increasing the $A\beta_{25–35}$ concentration almost 10 times at the condition without the lipids.

The same structural changes were observed in full-length $A\beta_{1–40}$ peptide. Investigations of the addition of lipid membranes to $A\beta_{1–42}$ and $A\beta_{1-40}$ under various pH and salt concentrations, however, concluded the peptide secondary structure being not the only factor in the membrane disrupting activity [93]. The additional NMR study of Aβ peptide binding to the lipid membranes showed no changes in lipid headgroup region conformation, and in the lipid chain flexibility and ordering [94]. The peptides therefore could appear to exist with lipid membranes in a non-interacting, or at least non-disturbing way at some conditions, while a severe disturbance may occur in other circumstances.

The questions of Aβ peptide interactions with membranes evolved in the necessity to differentiate between the incorporation and adsorption of peptides to the lipid membrane. The investigations of conformational changes in the Aβ structure over the time period of 18 days have shown that incorporated peptides avoid the conformational changes, while the surface associated Aβ peptides show dramatic changes by going from disordered structures to predominantly β-sheet structures after several weeks [95]. The mechanisms of these changes are however yet to be understood. A great deal of detailed information needed for shedding more light on the problem may perhaps come from theoretical studies based on molecular dynamics (MD) simulations.

In view of the continuous development of high-performance heterogeneous computing systems, the efficiency of MD methods for modeling the biological structures, such as lipid membranes and proteins interacting with them, is steadily increasing. MD simulations help to interpret and corroborate experimental data

obtained from SANS, SAND, NR, and INS discussed earlier as well as many other experimental techniques. In turn, the experimental results are an essential part in the verification and further improvements of MD force fields. Nowadays, one of the popular areas of the joined MD-experimental approaches is the study of the interaction of the Aβ peptide with model lipid membranes. The principal interest in this direction, registering particularly with MD methodology, is the problem of searching conformations and location of the Aβ peptide in membrane-water systems.

The replica–exchange molecular dynamics (REMD) and the umbrella sampling simulation methods are often used to solve the above problems [96–98]. The idea of the replica exchange method is that a set of replicas is created, each of which is assigned a certain temperature value, and those replicas are simulated further in parallel with a periodic exchange of conformational states. Umbrella sampling is one of the accelerated sampling methods, the idea of which is to insert an additional potential reducing potential barriers, that allows the system to bypass the conformational space more easily, and then the effect of this potential is subtracted from the obtained free energy profile. Well-tempered metadynamics is also a method of enhanced sampling and calculating the free energy landscape, which is accelerated by the bias potential depending on collective variables.

The first step towards investigating the mutual influence of Aβ peptides and lipid membranes is modeling systems with peptide monomers. Currently, a number of MD simulations have been carried out. They are aimed at studying the Aβ interaction with model membranes depending on the length and conformation of the peptide, as well as the composition of the bilayer (e.g., saturated or unsaturated lipid chains, zwitterionic or anionic lipid headgroups, cholesterol or melatonin addition, etc.). A general pattern of the Aβ interaction with lipid membranes is then justified by the consistency of results.

Simulations of the $A\beta_{25–35}$ monomer in an implicit water-membrane environment and explicit DMPC membrane with water models by REMD have shown for example that the peptide can locate in the membrane in two states – a surface-bound state and a less stable inserted state, between which Aβ can often be interconverted (see Fig. 10.10 for the illustration) [99, 100]. It is encouraging to recall similar conclusions achieved based on the SAND experiments [76], though the capability of MD expands

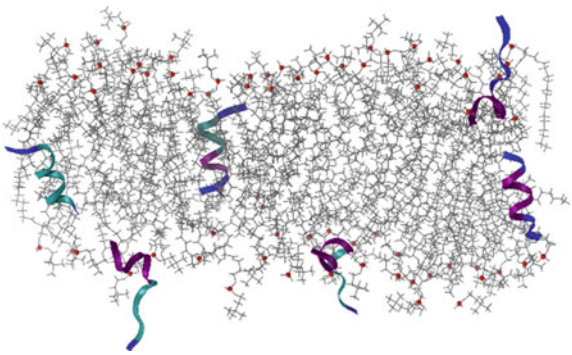

Fig. 10.10 Snapshots of $A\beta_{25–35}$ conformations (helix shown by purple, turn by cyan, and coil by blue colors) and positions in phospholipid membrane (phosphorus atoms shown by red points, rest of the lipids shown by gray color; water was omitted for the clarification of presentation)

the results further. Accordingly, the peptide has highly extended conformations in the surface-bound state. In the second state, the C-terminus has a stable helix shape and is located deep in the membrane, while the N-terminus is more disordered with lower helix propensities and closer to hydrophilic heads. In addition, the peptide binding slightly decreases membrane thickness and does not cause strong lipid disordering.

The REMD simulations of $A\beta_{10–40}$ monomer with an explicit DMPC bilayer demonstrate the existence of one stable peptide state in the membrane, in which the C-terminus penetrates the hydrophobic part of phospholipids and forms a stable helix, while the N-terminus interacts mainly with the bilayer surface [101]. At the same time, the membrane thickness and area per lipid are significantly reduced, though the increase in the disorder of lipid tails is insignificant due to the shallow insertion of $A\beta_{10–40}$.

The results obtained by umbrella sampling simulations of the $A\beta_{1–42}$ peptide in zwitterionic DPPC and anionic DOPS bilayers, and molecular dynamics simulations of the $A\beta_{1–40}$ in zwitterionic POPC, anionic POPS, and mixed POPC/POPE bilayers suggest that the anionic bilayers may stabilize the peptide secondary structure to a greater extent than the zwitterionic ones. Besides, the C-terminus is embedded into the membrane hydrophobic core in all but the case of anionic membranes, while the N-terminus is located closer to the water-membrane interface and more strongly exposed to a solvent [44, 102]. The main $A\beta_{1–40}$ conformations are helices and random coils, although β-hairpins are also observed, mainly in N-terminus peptide region.

The composition of lipid bilayers significantly influences the insertion, orientation, and aggregation of Aβ peptides, regulating Aβ-membrane interactions. Polyunsaturated lipids (PUL) cause, apparently, stronger adsorption of Aβ on the membrane and lead to a weaker binding between peptides in aggregates [9]. In the presence of cholesterol in the lipid membrane, that has been discussed above to ensure a stiffened membrane as opposed to the highly fluid PUL membranes, the $A\beta_{25–35}$ peptide does not permeate into the bilayer hydrophobic core due to the high order of lipids. This leads to the peptide aggregation on the membrane surface and a slight decrease of the bilayer thickness [103, 104]. In the case of the longer $A\beta_{1–40}$ and $A\beta_{1–42}$ peptides, $A\beta_{1–40}$ also ends up preferably at the surface of cholesterol-depleted membranes, though it exhibits a partially or completely embedded state in cholesterol-enriched membranes. In turn, $A\beta_{1–42}$ peptide inserts partially or completely into cholesterol-depleted membranes and completely inserts into cholesterol-enriched membranes [105].

10.8 Concluding Remarks

Alzheimer's disease was first described in 1906 based on its clinical symptoms and microscopic changes in the brain structure [106]. For many years then to come, microscopy was the main method for recognizing the disease at the autopsy of patients. With its increasing social impact, however, increased also an interest in

its identification. Over more than a century, it has seen a huge development in the research approaches available more or less readily for its interrogation.

The research in general and structural biophysics in particular, have proven to benefit from the development of dedicated X-ray sources. Starting with the fixed tube, coincidently around the same time as the AD was identified, all the way to the free electron lasers, their brilliance has advanced by impressive 16 orders of magnitude. The golden era of neutrons following its discovery in 1932, brought other expectations and advancements. The peculiar properties of neutrons allowed for building sample holders capable to reproduce biologically relevant conditions during experiments. The *in situ* approaches expanded to include contrast variation and deuterium labeling techniques as the most powerful tools. The increase of computational power, doubling every 2 years, earned theoretical approaches their niche in structural biology most recently. MD simulations, following the sample dynamics for microseconds now, provide an unprecedented level and amount of details. We have entered a century of big data, built on promises to combine all the information into one model.

The research on AD may not be at the end just yet, but we certainly have a lot of knowledge by now. Owing to the advancements in research approaches, there is a final number of hypotheses describing the origin of the disease. There is a final amount of models depicting the interactions leading to the onset of the disease. Most importantly though, there is finally a limited number of proposals for combating the disease. Some of the discussed problems certainly find their place at the membrane, either as the place of origin, development, or even action of Aβ peptides. The closer and closer looks at these problems will undoubtedly provide an understanding of relevant mechanisms and perhaps will be a part of the final solution.

Acknowledgements This work has been supported by the Russian Science Foundation under grant 19-72-20186.

References

1. Lodish H, Arnold B, Zipursky L, Matsudaira P, Baltimore D, Darnell J (1999) Molecular Cell Biology, 4th edn. W. H. Freeman, New York
2. Lee AG (2004) How lipids affect the activities of integral membrane proteins. Biochim Biophys Acta - Biomembr 1666:62–87
3. Van Meer G, Voelker DR, Feigenson GW (2008) Membrane lipids: where they are and how they behave. Nat Rev Mol Cell Biol 9:112–124
4. Koynova R, Caffrey M (1998) Phases and phase transitions of the phosphatidylcholines. Biochim. Biophys Acta - Rev Biomembr 1376:91–145
5. Tardieu A, Luzzati V, Reman FC (1973) Structure and polymorphism of the hydrocarbon chains of lipids: a study of lecithin-water phases. J Mol Biol 75:711–733
6. Chapman D (1975) Phase transitions and fluidity characteristics of lipids and cell membranes. Q Rev Biophys 8:185–235
7. Bretscher MS, Munro S (1993) Cholesterol and the Golgi apparatus. Science 261:1280–1281

8. Drolle E et al (2013) Effect of melatonin and cholesterol on the structure of DOPC and DPPC membranes. Biochim Biophys Acta - Biomembr 1828:2247–2254
9. Ntarakas N, Ermilova I, Lyubartsev A (2019) Effects of lipid saturation on amyloid-beta peptides partitioning and aggregation in neuronal membranes: molecular dynamics simulations. Eur Biophys J 48:813–824
10. Martel A et al (2017) Membrane permeation versus amyloidogenicity: a multitechnique study of islet amyloid polypeptide interaction with model membranes. J Am Chem Soc 139:137–148
11. Dante S, Hauß T, Brandt A, Dencher NA (2008) Membrane fusogenic activity of the Alzheimer's peptide Aβ(1–42) demonstrated by small-angle neutron scattering. J Mol Biol 376:393–404
12. Prince M, Comas-Herrera A, Knapp M, Guerchet M, Karagiannidou M (2016) World Alzheimer report 2016: improving healthcare for people living with dementia: coverage, quality and costs now and in the future
13. Hippius H, Neundörfer G (2003) The discovery of Alzheimer's disease. Dialogues Clin Neurosci 5:101–108
14. Liu PP, Xie Y, Meng XY, Kang JS (2019) History and progress of hypotheses and clinical trials for Alzheimer's disease. Signal Transduct Target Ther 4:29
15. Bush AI et al (1994) Rapid induction of Alzheimer Aβ amyloid formation by zinc. Science 265:1464–1467
16. Spinello A, Bonsignore R, Barone G, K. Keppler B, Terenzi A (2016) Metal ions and ietal complexes in Alzheimer's Disease. Curr Pharm Des 22:3996–4010
17. Clements A, Allsop D, Walsh DM, Williams CH (1996) Aggregation and metal-binding properties of mutant forms of the amyloid Aβ peptide of Alzheimer's disease. J Neurochem 66:740–747
18. Francis PT, Palmer AM, Snape M, Wilcock GK (1999) The cholinergic hypothesis of Alzheimer's disease: a review of progress. J Neurol Neurosurg Psychiatry 66:137–147
19. Mudher A, Lovestone S (2002) Alzheimer's disease – do tauists and baptists finally shake hands? Trends Neurosci 25:22–26
20. Hardy J, Allsop D (1991) Amyloid deposition as the central event in the aetiology of Alzheimer's disease. Trends Pharmacol Sci 12:383–388
21. Martorana A, Esposito Z, Koch G (2010) Beyond the cholinergic hypothesis: do current drugs work in Alzheimer's disease? CNS Neurosci Ther 16:235–245
22. Nussbaum JM, Seward ME, Bloom GS (2013) Alzheimer disease. Prion 7:14–19
23. Mohandas E, Rajmohan V, Raghunath B (2009) Neurobiology of Alzheimer's disease. Indian J Psychiatry 51:55–61
24. Di J, Cohen LS, Corbo CP, Phillips GR, El Idrissi A, Alonso AD (2016) Abnormal tau induces cognitive impairment through two different mechanisms: Synaptic dysfunction and neuronal loss. Sci Rep 6:1–12
25. Hardy J, Selkoe DJ (2002) The amyloid hypothesis of Alzheimer's disease: progress and problems on the road to therapeutics. Science 297:353–356
26. Vestergaard M, Hamada T, Takagi M (2008) Using model membranes for the study of amyloid beta:lipid interactions and neurotoxicity. Biotechnol Bioeng 99:753–763
27. Buchsteiner A, Hauß T, Dante S, Dencher NA (2010) Alzheimer's disease amyloid-B peptide analogue alters the PS-dynamics of phospholipid membranes. Biochim Biophys Acta - Biomembr 1798:1969–1976
28. Ehehalt R, Keller P, Haass C, Thiele C, Simons K (2003) Amyloidogenic processing of the Alzheimer beta-amyloid precursor protein depends on lipid rafts. J Cell Biol 160:113–123
29. Hattori C et al (2006) BACE1 interacts with lipid raft proteins. J Neurosci Res 84:912–917
30. Sadigh-Eteghad S, Talebi M, Farhoudi M, Golzari SEJ, Sabermarouf B, Mahmoudi J (2014) Beta-amyloid exhibits antagonistic effects on alpha 7 nicotinic acetylcholine receptors in orchestrated manner. J Med Hypotheses Ideas 8:49–52
31. Yao ZX, Papadopoulos V (2002) Function of beta-amyloid in cholesterol transport: a lead to neurotoxicity. FASEB J 16:1677–1679

32. Bogoyevitch MA, Boehm I, Oakley A, Ketterman AJ, Barr RK (2004) Targeting the JNK MAPK cascade for inhibition: basic science and therapeutic potential. In: Biochimica et Biophysica Acta - Proteins and Proteomics. Elsevier, pp 89–101
33. Soscia SJ, et al (2010) The Alzheimer's disease-associated amyloid β-Protein is an antimicrobial peptide. PLoS One 5:e9505
34. Dahlgren KN, Manelli AM, Stine WB, Baker LK, Krafft GA, LaDu MJ (2002) Oligomeric and fibrillar species of amyloid-β peptides differentially affect neuronal viability. J Biol Chem 277:32046–32053
35. Kim H-S et al (2002) Amyloid beta peptide induces cytochrome C release from isolated mitochondria. NeuroReport 13:1989–1993
36. Lim L, Wenk MR (2009) Neuronal membrane lipids–their role in the synaptic vesicle cycle. Handbook of neurochemistry and molecular neurobiology. Springer, US, Boston, pp 223–238
37. Chu N, Kučerka N, Liu Y, Tristram-Nagle S, Nagle JF (2005) Anomalous swelling of lipid bilayer stacks is caused by softening of the bending modulus. Phys Rev E 71:41904
38. Ermilova I, Lyubartsev AP (2019) Cholesterol in phospholipid bilayers: positions and orientations inside membranes with different unsaturation degrees. Soft Matter 15:78–93
39. Kučerka N, Marquardt D, Harroun TA, Nieh M-P, Wassall SR, Katsaras J (2009) The functional significance of lipid diversity: orientation of cholesterol in bilayers is determined by lipid species. J Am Chem Soc 131:16358–16359
40. Martinez-Seara H, Róg T, Pasenkiewicz-Gierula M, Vattulainen I, Karttunen M, Reigada R (2008) Interplay of unsaturated phospholipids and cholesterol in membranes: effect of the double-bond position. Biophys J 95:3295–3305
41. Nagle JF, Tristram-Nagle S (2000) Structure of lipid bilayers. Biochim Biophys Acta - Rev Biomembr 1469:159–195
42. Petrache HI, Gouliaev N, Tristram-Nagle S, Zhang R, Suter RM, Nagle JF (1998) Interbilayer interactions from high-resolution x-ray scattering. Phys Rev E 57:7014–7024
43. Yoda M, Miura T, Takeuchi H (2008) Non-electrostatic binding and self-association of amyloid β-peptide on the surface of tightly packed phosphatidylcholine membranes. Biochem Biophys Res Commun 376:56–59
44. Davis CH, Berkowitz ML (2009) Interaction between amyloid-β (1–42) peptide and phospholipid bilayers: A molecular dynamics study. Biophys J 96:785–797
45. Kirkitadze MD, Condron MM, Teplow DB (2001) Identification and characterization of key kinetic intermediates in amyloid β-protein fibrillogenesis. J Mol Biol 312:1103–1119
46. Kobayashi S, Tanaka Y, Kiyono M, Chino M, Chikuma T, Hoshi K, Ikeshima H (2015) Dependence pH and proposed mechanism for aggregation of Alzheimer's disease-related amyloid-β(1–42) protein. J Mol Struct 1094:109–117
47. Butterfield DA, Lauderback CM (2002) Lipid peroxidation and protein oxidation in Alzheimer's disease brain: potential causes and consequences involving amyloid β-peptide-associated free radical oxidative stress. Free Radic Biol Med 32:1050–1060
48. Butterfield DA, Boyd-Kimball D (2004) Amyloid β-peptide(1–42) contributes to the oxidative stress and neurodegeneration found in Alzheimer disease brain. Brain Pathol Int Soc Neuropathol 14:426–432
49. Marcus D et al (1998) Increased peroxidation and reduced antioxidant enzyme activity in Alzheimer's disease. Exp Neurol 150:40–44
50. Hensley K et al (1995) Brain regional correspondence between Alzheimer's disease histopathology and biomarkers of protein oxidation. J Neurochem 65:2146–2156
51. Cheignon C, Tomas M, Bonnefont-Rousselot D, Faller P, Hureau C, Collin F (2018) Oxidative stress and the amyloid beta peptide in Alzheimer's disease. Redox Biol 14:450–464
52. Quincke G (1888) Ueber periodische Ausbreitung an Flüssigkeitsoberflächen und dadurch hervorgerufene Bewegungserscheinungen. Ann der Phys und Chemie 271:580–642
53. Pabst G, Kučerka N, Nieh MP, Rheinstädter MC, Katsaras J (2010) Applications of neutron and X-ray scattering to the study of biologically relevant model membranes. Chem Phys Lipids 163:460–479

54. Marquardt D, Heberle FA, Nickels JD, Pabst G, Katsaras J (2015) On scattered waves and lipid domains: detecting membrane rafts with X-rays and neutrons. Soft Matter 11:9055–9072
55. Knoll W, Haas J, Stuhrmann HB, Füldner H-H, Vogel H, Sackmann E (1981) Small-angle neutron scattering of aqueous dispersions of lipids and lipid mixtures. A contrast variation study. J Appl Crystallogr 14:191–202
56. Murugova TN et al (2011) Potentials of small-angle neutron scattering for studies of the structure of "live" mitochondria. Neutron News 22:11–14
57. Armstrong CL et al (2012) Co-existence of gel and fluid lipid domains in single-component phospholipid membranes. Soft Matter 8:4687–4694
58. Kuklin A et al (2020) On the origin of the anomalous behavior of lipid membrane properties in the vicinity of the chain-melting phase transition. Sci Rep 10:1–8
59. Luzzati V, Tardieu A (1974) Lipid phases: structure and structural transitions. Annu Rev Phys Chem 25:79–94
60. Lewis R, McElhaney R (2011) The mesomorphic phase behavior of lipid bilayers. In: The structure of biological membranes, 3rd edn, pp 19–89. CRC Press, Cambridge
61. Tolédano JC, Tolédano P (1987) The Landau theory of magnetic phase transitions. World Sci Lecture Notes Phys C 3:307–373
62. Kittel C, Kroemer H, Scott HL (1998) Thermal physics, 2nd ed. Am J Phys 66:164–167
63. Nagle JF (1973) Lipid bilayer phase transition: density measurements and theory. Proc Natl Acad Sci U S A 70:3443–3444
64. Kratky O, Leopold H, Stabinger H (1973) [5] The determination of the partial specific volume of proteins by the mechanical oscillator technique. Methods Enzymol 27:98–110
65. Murugova TN, Balgavý P (2014) Molecular volumes of DOPC and DOPS in mixed bilayers of multilamellar vesicles. Phys Chem Chem Phys 16:18211–18216
66. Murugova T et al (2020) Structural changes introduced by cholesterol and melatonin to the model membranes mimicking preclinical conformational diseases. Gen Physiol Biophys 39:135–144
67. Lau TL et al (2006) Amyloid-β peptide disruption of lipid membranes and the effect of metal ions. J Mol Biol 356:759–770
68. Kučerka N, Liu Y, Chu N, Petrache HI, Tristram-Nagle S, Nagle JF (2005) Structure of fully hydrated fluid phase DMPC and DLPC lipid bilayers using X-Ray scattering from oriented multilamellar arrays and from unilamellar vesicles. Biophys J 88:2626–2637
69. Kuklin AI, et al (2017) Neutronographic investigations of supramolecular structures on upgraded small-angle spectrometer YuMO. J Phys Conf Ser 848:012010. Institute of Physics Publishing
70. Sreij R et al (2018) DMPC vesicle structure and dynamics in the presence of low amounts of the saponin aescin. Phys Chem Chem Phys 20:9070–9083
71. Kučerka N, Nagle JF, Feller SE, Balgavý P (2004) Models to analyze small-angle neutron scattering from unilamellar lipid vesicles. Phys Rev E - Stat Physics, Plasmas, Fluids, Relat Interdiscip Top 69:9
72. Puglielli L, Tanzi RE, Kovacs DM (2003) Alzheimer's disease: the cholesterol connection
73. Karasek M (2004) Melatonin, human aging, and age-related diseases. Exp Gerontol 39:1723–1729
74. Kučerka N, Nieh M, Pencer J, Sachs J, Katsaras J (2009) What determines the thickness of a biological membrane. Gen Physiol Biophys 28:117–125
75. Sears VF (1992) Neutron scattering lengths and cross sections. Neutron News 3:26–37
76. Barrett M, Alsop R, Hauß T, Rheinstädter M (2015) The position of Aβ22-40 and Aβ1-42 in anionic lipid membranes containing cholesterol. Membranes (Basel) 5:824–843
77. Dante S, Hauss T, Dencher NA (2002) β-amyloid 25 to 35 is intercalated in anionic and zwitterionic lipid membranes to different extents. Biophys J 83:2610–2616
78. Hrubovčák P et al (2018) Location of the general anesthetic n-decane in model membranes. J Mol Liq 276:624–629

79. Dante S, Hauß T, Steitz R, Canale C, Dencher NA (2011) Nanoscale structural and mechanical effects of beta-amyloid (1–42) on polymer cushioned membranes: a combined study by neutron reflectometry and AFM Force Spectroscopy. Biochim Biophys Acta - Biomembr 1808:2646–2655
80. Hellstrand E et al (2013) Adsorption of α-synuclein to supported lipid bilayers: Positioning and role of electrostatics. ACS Chem Neurosci 4:1339–1351
81. Jackson AJ (2008) Introduction to small-angle neutron scattering and neutron reflectometry. NIST Center for Neutron Research. https://ftp.ncnr.nist.gov/summerschool/ss10/pdf/SANS_NR_Intro.pdf
82. Maierhofer AP, Bucknall DG, Bayerl TM (2000) Modulation of cytochrome C coupling to anionic lipid monolayers by a change of the phase state: a combined neutron and infrared reflection study. Biophys J 79:1428–1437
83. Lu JR, Murphy EF, Su TJ, Lewis AL, Stratford PW, Satija SK (2001) Reduced protein adsorption on the surface of a chemically grafted phospholipid monolayer. Langmuir 17:3382–3389
84. Rondelli V et al (2016) Amyloid β Peptides in interaction with raft-mime model membranes: a neutron reflectivity insight. Sci Rep 6:20997
85. Baron Alfred QR (2016) High-Resolution Inelastic X-Ray scattering I: Context, spectrometers, samples, and superconductors. In: Jaeschke Eberhard J, Khan Shaukat, Schneider Jochen R, Hastings Jerome B (eds) Synchrotron light sources and free-electron lasers. Springer, Cham, pp 1643–1719. https://doi.org/10.1007/978-3-319-14394-1_41
86. Bonn M, Bakker HJ, Ghosh A, Yamamoto S, Sovago M, Campen RK (2010) Structural inhomogeneity of interfacial water at lipid monolayers revealed by surface-specific vibrational pump-probe spectroscopy. J Am Chem Soc 132:14971–14978
87. Mashaghi A et al (2012) Interfacial water facilitates energy transfer by inducing extended vibrations in membrane lipids. J Phys Chem B 116:6455–6460
88. Busch S, Smuda C, Pardo LC, Unruh T (2010) Molecular mechanism of long-range diffusion in phospholipid membranes studied by quasielastic neutron scattering. J Am Chem Soc 132:3232–3233
89. Pronk S, Lindahl E, Kasson PM (2015) Coupled diffusion in lipid bilayers upon close approach. J Am Chem Soc 137:708–714
90. Zhernenkov M et al (2016) Revealing the mechanism of passive transport in lipid bilayers via phonon-mediated nanometre-scale density fluctuations. Nat Commun 7:11575–11575
91. Soloviov D et al (2020) Functional lipid pairs as building blocks of phase-separated membranes. Proc Natl Acad Sci U S A 117:4749–4757
92. Terzi E, Seelig J, Hölzemann G (1994) Alzheimer β-Amyloid peptide 25–35: electrostatic interactions with phospholipid membranes. Biochemistry 33:7434–7441
93. McLaurin JA, Chakrabartty A (1997) Characterization of the interactions of Alzheimer β-amyloid peptides with phospholipid membranes. Eur J Biochem 245:355–363
94. Terzi E, Hölzemann G, Seelig J (1997) Interaction of Alzheimer β-amyloid peptide(1–40) with lipid membranes. Biochemistry 36:14845–14852
95. Bokvist M, Lindström F, Watts A, Gröbner G (2004) Two types of Alzheimer's β-Amyloid (1–40) peptide membrane interactions: aggregation preventing transmembrane anchoring versus accelerated surface fibril formation. J Mol Biol 335:1039–1049
96. Sugita Y, Okamoto Y (1999) Replica-exchange molecular dynamics method for protein folding. Chem Phys Lett 314:141–151
97. Torrie GM, Valleau JP (1977) Nonphysical sampling distributions in Monte Carlo free-energy estimation: umbrella sampling. J Comput Phys 23:187–199
98. Barducci A, Bussi G, Parrinello M (2008) Well-tempered metadynamics: A smoothly converging and tunable free-energy method. Phys Rev Lett 100:020603
99. Smith AK, Klimov DK (2018) Binding of cytotoxic Aβ25-35 peptide to the dimyristoylphosphatidylcholine lipid bilayer. J Chem Inf Model 58:1053–1065
100. Tsai HHG, Bin LJ, Tseng SS, Pan XA, Shih YC (2010) Folding and membrane insertion of amyloid-beta (25–35) peptide and its mutants: Implications for aggregation and neurotoxicity. Proteins Struct Funct Bioinforma 78:1909–1925

101. Lockhart C, Klimov DK (2014) Alzheimer's Aβ10-40 peptide binds and penetrates DMPC bilayer: an isobaric-isothermal replica exchange molecular dynamics study. J Phys Chem B 118:2638–2648
102. Lemkul JA, Bevan DR (2011) Lipid composition influences the release of Alzheimer's amyloid β-peptide from membranes. Protein Sci 20:1530–1545
103. Ermilova I, Lyubartsev AP (2020) Modelling of interactions between Aβ(25–35) peptide and phospholipid bilayers: effects of cholesterol and lipid saturation. RSC Adv 10:3902–3915
104. Ivankov OI et al (2020) Interactions in the model membranes mimicking preclinical conformational diseases. Adv Biomembr Lipid Self-Assembly 31:185–214
105. Qiu L, Buie C, Reay A, Vaughn MW, Cheng KH (2011) Molecular dynamics simulations reveal the protective role of cholesterol in β-amyloid protein-induced membrane disruptions in neuronal membrane mimics. J Phys Chem B 115:9795–9812
106. Alzheimer A (1907) Über eine eigenartige Erkrankung der Hirnrinde [article in German]. Allg Z Psych Psych-gerich Med 64:146–148
107. Pavol H, Ermuhammad D, Tomáš K, Oleksandr T, Kholmirzo K, Norbert K Reflectometry and molecular dynamics study of the impact of cholesterol and melatonin on model lipid membranes. Eur Biophys J. https://doi.org/10.1007/s00249-021-01564-y